

# Chemistry and Biology of Aflatoxin-DNA Adducts

Michael P. Stone\*, Surajit Banerjee, Kyle L. Brown, and Martin Egli

Department of Chemistry, Center in Molecular Toxicology, Vanderbilt-Ingram Cancer Center, Vanderbilt University, Nashville, TN 37235

*Aspergillus flavus* is a fungal contaminant of stored rice, wheat, corn, and other grainstuffs, and peanuts. This is of concern to human health due to the fact that the fungus produces the mycotoxin aflatoxin B<sub>1</sub> (AFB<sub>1</sub>), which is genotoxic and is implicated in the etiology of human liver cancer. AFB<sub>1</sub> is oxidized by cytochrome P450 to form aflatoxin B<sub>1</sub> epoxide, which forms an N7-dG adduct (AFB<sub>1</sub>-N7-dG) in DNA. The latter rearranges to a formamidopyrimidine (AFB<sub>1</sub>-FAPY) derivative that equilibrates between  $\alpha$  and  $\beta$  anomers of the deoxyribose. In DNA, both the AFB<sub>1</sub>-N7-dG and AFB<sub>1</sub>- $\beta$ -FAPY adducts intercalate above the 5'-face of the damaged guanine. Each produces G→T transversions in *Escherichia coli*, but the AFB<sub>1</sub>- $\beta$ -FAPY adduct is more mutagenic. The *Sulfolobus solfataricus* P2 DNA polymerase IV (Dpo4) provides a model

for understanding error-prone bypass of the AFB<sub>1</sub>-N7-dG and AFB<sub>1</sub>-β-FAPY adducts. It bypasses the AFB<sub>1</sub>-N7-dG adduct, but it conducts error-prone replication past the AFB<sub>1</sub>-FAPY adduct, including mis-insertion of dATP, consistent with the G→T mutations characteristic of AFB<sub>1</sub> mutagenesis in *E. coli*. Crystallographic analyses of a series of binary and ternary complexes with the Dpo4 polymerase revealed differing orientations of the N7-C8 bond of the AFB<sub>1</sub>-N7-dG adduct as compared to the N<sup>5</sup>-C8 bond in the AFB<sub>1</sub>-β-FAPY adduct, and differential accommodation of the intercalated AFB<sub>1</sub> moieties within the active site. These may modulate AFB<sub>1</sub> lesion bypass by this polymerase.

## Introduction

The fungi *Aspergillus flavus* is a frequent contaminant of stored rice, wheat, corn, and other grainstuffs, and peanuts. This is of serious concern to human health due to the fact that the fungus produces the mycotoxin aflatoxin B<sub>1</sub> (AFB<sub>1</sub>) (1-4). This mycotoxin is among the most genotoxic natural products and it is mutagenic in bacteria (2, 5-7), tumorigenic in fish (8, 9), carcinogenic in rodents (10, 11), and is implicated in the etiology of human liver cancer (12-14). Aflatoxin exposures are implicated in mutations to the p53 tumor suppressor gene (15-21).

## Chemistry of AFB<sub>1</sub>-Induced Alkylation of DNA

The genotoxicity of AFB<sub>1</sub> is associated with its oxidation to the reactive electrophile AFB<sub>1</sub>-*exo*-8,9-epoxide by cytochromes P450 (Chart 1) (22-26). The synthesis of AFB<sub>1</sub>-*exo*-8,9-epoxide was reported by Baertschi et al. (27) and involved oxidation of AFB<sub>1</sub> with dimethyldioxirane (28, 29). The availability of this epoxide facilitated investigations with respect to both the chemical and biological consequences of AFB<sub>1</sub>-induced DNA alkylation. The short-lived AFB<sub>1</sub>-*exo*-8,9-epoxide (26) reacts efficiently with duplex DNA to yield the AFB<sub>1</sub> N7-dG adduct *trans*-8,9-dihydro-8-(N7-guanyl)-9-hydroxyaflatoxin B<sub>1</sub> (2, 30). This is attributed to intercalation of the epoxide above the 5' face of dG in DNA (31), facilitating nucleophilic attack by the N7 nitrogen at the C8 carbon of the epoxide (32). At acidic pH, the AFB<sub>1</sub>-N7-dG adduct depurinates to yield a potentially genotoxic abasic site. In contrast, hydrolysis of the guanine imidazole ring forms the AFB<sub>1</sub> formamidopyrimidine adduct (AFB<sub>1</sub>-FAPY) (33). In DNA, the AFB<sub>1</sub>-FAPY adduct is longer-lived (34-36). Smela et al. (37) demonstrated that an oligodeoxynucleotide containing an AFB<sub>1</sub>-FAPY adduct

equilibrated between two separable species, one of which was mutagenic whereas the other blocked DNA replication. These correspond to the  $\alpha$  and  $\beta$  anomers of the AFB<sub>1</sub>-FAPY adduct; the mutagenic species is the AFB<sub>1</sub>- $\beta$ -FAPY adduct; the AFB<sub>1</sub>- $\alpha$ -FAPY adduct blocks replication (Chart 2) (38). In duplex DNA the AFB<sub>1</sub>- $\beta$ -FAPY anomer is favored, but in single strand DNA, a 2:1  $\alpha$ : $\beta$  equilibrium mixture of anomers is observed (38). Additionally, the AFB<sub>1</sub>-FAPY adduct undergoes conformational rearrangements involving atropisomers about the C5-N5 bond and geometrical isomers of the formyl moiety (38). Note the change in numbering in going from the AFB<sub>1</sub>-N7-dG adduct to the AFB<sub>1</sub>-FAPY adduct; the C5-N5 bond in the AFB<sub>1</sub>-FAPY adduct corresponds to the C5-N7 bond in the AFB<sub>1</sub>-N7-dG adduct.

### **Site-Specific Mutagenesis of the AFB<sub>1</sub>-N7-dG Adduct in *E. coli***

Essigmann and co-workers had developed methodology allowing individual DNA adducts, such as those induced by exposures to AFB<sub>1</sub>-*exo*-8,9-epoxide, to be situated at defined sites in the *E. coli* virus M13mp8 (39). These site-specifically modified phage genomes could then be introduced into *E. coli*, where replication would occur, subject to the actions of both replication and repair enzymes endogenous to the bacterium. By assessing the levels and types of DNA sequence alteration(s) induced in progeny phage at the site originally occupied by the adducts, a detailed picture of the cellular processing of these adducts by *E. coli* emerged (39). Such site-specific mutagenesis assays demonstrated that the AFB<sub>1</sub>-N7-dG adduct was mutagenic in *E. coli*, yielding primarily G→T transversions at levels of about 5% (40). This observation was particularly significant because earlier studies had indicated that G→T transversions were the primary mutations associated with random AFB<sub>1</sub> mutagenesis in *E. coli* (6). Consequently, these site-specific mutagenesis data (40) implicated the AFB<sub>1</sub>-N7-dG adduct as a pre-mutagenic lesion induced by AFB<sub>1</sub> in *E. coli*.

### **Structural Studies of the AFB<sub>1</sub>-N7-dG Adduct in Oligodeoxynucleotides**

Using standard NMR methodology (41, 42), structures of oligodeoxynucleotide duplexes containing AFB<sub>1</sub> N7-dG adducts were obtained by our laboratory. These revealed the basis by which the AFB<sub>1</sub> N7-dG adduct was accommodated within duplex DNA. The AFB<sub>1</sub>-N7-dG adduct intercalated above the 5' face of the modified dG in two oligodeoxynucleotides: d(ATCXAT)•d(ATCGAT), as shown in Figure 1, X = AFB<sub>1</sub>-N7-dG adduct, and d(ATXCAT)<sub>2</sub> (43-45). A structure of the AFB<sub>1</sub> N7-dG adduct in an oligodeoxynucleotide duplex containing an extra dA opposite the AFB<sub>1</sub> moiety

was also obtained (46). A structurally-related adduct of sterigmatocystin formed a similar intercalated structure (47). Unlike most DNA adducts, the AFB<sub>1</sub> N7-dG adducts thermodynamically stabilized the DNA duplex, as evidenced by increases in duplex melting temperatures (T<sub>m</sub> studies), as monitored either by UV spectroscopy or by NMR (48, 49). These structural and thermodynamic observations provide insight into the structural alterations of the DNA duplex that may modulate the repair of AFB<sub>1</sub> lesions, and have led to the suggestion that the AFB<sub>1</sub> N7-dG adduct may be refractory to DNA repair (49). Whether this is indeed the case but this remains to be established. It is established that the AFB<sub>1</sub>-N7-dG adduct is a substrate for nucleotide excision repair (50). Significantly, DNA damage frequently involves the "flipping" of damaged bases into an active site pocket of the repair enzyme, particularly in the case of base excision repair (51), but possibly also in the case of nucleotide excision repair (52). One can speculate that an intercalated and thermodynamically stabilizing adduct might be more difficult to recognize and repair.

### **Site-Specific Mutagenesis of the AFB<sub>1</sub>-FAPY Adduct in *E. coli***

Opening of the imidazole ring of the initially formed cationic AFB<sub>1</sub>-N7-dG adduct (2, 30) yields the AFB<sub>1</sub>-β-FAPY adduct (33, 38). Site-specific mutagenesis experiments carried out by Essigmann and co-workers revealed that the AFB<sub>1</sub>-β-FAPY adduct yielded G→T transversions at levels as high as 36% in *E. coli* (37), significantly higher than those observed for the cationic AFB<sub>1</sub>-N7-dG adduct (40). This observation, combined with observations that the AFB<sub>1</sub>-β-FAPY adduct was persistent *in vivo* (34-36), suggested that the AFB<sub>1</sub>-β-FAPY adduct may be the most genotoxic lesion formed by exposures to AFB<sub>1</sub>. In single strand DNA, the lack of the complementary strand facilitates the epimerization of the deoxyribose and the formation of an equilibrium mixture of α and β FAPY anomers, with the α anomer predominating in this sequence context (37). In *E. coli*, the AFB<sub>1</sub>-α-FAPY adduct was a block to replication (37).

### **Structural Studies of the AFB<sub>1</sub>-FAPY Adducts in Oligodeoxynucleotides**

As shown in Figure 2, in DNA the AFB<sub>1</sub>-β-FAPY adduct intercalated with the AFB<sub>1</sub> moiety on the 5' face of the pyrimidine moiety of the adducted nucleotide (49, 53), similar to the initially formed AFB<sub>1</sub>-N7-dG adduct (43, 44, 46, 54). The stability of the AFB<sub>1</sub>-β-FAPY adduct in DNA was attributed to robust interstrand stacking interactions (49, 53). The AFB<sub>1</sub>-α-FAPY adduct also intercalated above the 5' face of the damaged base (55). The lower stability of the AFB<sub>1</sub>-α-FAPY as compared to the AFB<sub>1</sub>-β-FAPY adduct (49, 53) was

attributed to structural perturbations in the DNA and reduced interstrand stacking (55). The similar 5'-intercalation of the AFB<sub>1</sub>-N7-dG (43, 44, 46, 54) and AFB<sub>1</sub>-β-FAPY (53) adducts were consistent with each producing G→T transversions in *E. coli*, but did not readily explain the increased mutagenicity of the AFB<sub>1</sub>-β-FAPY adduct (37).

### **Bypass of AFB<sub>1</sub> Adducts by the *Sulfolobus solfataricus* P2 DNA polymerase IV (Dpo4)**

In an effort to understand why the AFB<sub>1</sub>-β-FAPY adduct is more mutagenic than is the AFB<sub>1</sub>-N7-dG adduct (37), we examined the bypass of the AFB<sub>1</sub>-N7-dG (43, 44, 46, 54) and AFB<sub>1</sub>-β-FAPY (53) adducts by the *Sulfolobus solfataricus* P2 DNA polymerase IV (Dpo4) (56), a DinB homologue (57). In one series of experiments, the 18-mer template 5'-d(TCATTXAAATCCTTCCCC)-3' (X = AFB<sub>1</sub>-N7-dG or AFB<sub>1</sub>-β-FAPY adduct) was annealed with the Sequence I 12-mer primer 5'-d(GGGGAAGGATT)-3', leading to a template•primer primed for incorporation of dNTPs opposite the adduct (Chart 3) (56). In a second series of experiments, the 18-mer template 5'-d(TCATTXAAATCCTTCCCC)-3' (X = AFB<sub>1</sub>-N7-dG or AFB<sub>1</sub>-β-FAPY adduct) was also annealed with the Sequence II 13-mer primer 5'-d(GGGGAAGGATTC)-3', leading to a template•primer primed for extension of dNTPs beyond the dX:dC primer terminus (Chart 3) (56).

Figure 3 (top panel) shows the results of single nucleotide incorporation assays using the Sequence I 18mer:12mer template:primer (Chart 3) (56). The Dpo4 polymerase exhibited a strong preference for the correct incorporation of dCTP opposite the AFB<sub>1</sub>-N7-dG lesion. When all four dNTPs were included in the reaction, the polymerase extended the primer to the full-length 18-mer product. Figure 3 (bottom panel) shows the results of single nucleotide incorporation assays using the Sequence II 18mer:13mer template:primer (Chart 3). This experiment monitored single nucleotide extension beyond the correctly inserted dC at the 3'-terminus of the primer. The polymerase correctly inserted dATP twice, corresponding to the positioning of the two thymines 5' to the AFB<sub>1</sub>-N7-dG lesion in the template. When all four dNTPs were included in the reaction, the polymerase extended the primer to the full-length 18-mer product.

Figure 4 (top panel) shows the results of single nucleotide incorporation assays using the Sequence I 18mer:12mer template:primer (Chart 3) (56). The Dpo4 polymerase was less efficient at inserting nucleotides opposite the AFB<sub>1</sub>-β-FAPY lesion. The correct nucleotide dCTP was inserted opposite the AFB<sub>1</sub>-β-FAPY lesion but the incorrect nucleotide dATP was also incorporated. In the dATP lanes, weak bands are observed corresponding to the 14-mer and 15-mer products, suggesting that multiple insertions of dATP occurred, presumably

involving the two 5'-neighboring template dT nucleotides in the template strand, perhaps coupled with strand slippage. Thus the AFB<sub>1</sub>-β-FAPY adduct exhibited both correct incorporation of dCTP and misincorporation of dATP for this template:primer. In the presence of all four dNTPs, the polymerase extended the primer to the full-length 18-mer product. Figure 4 (bottom panel) shows the results of single nucleotide incorporation assays using the Sequence II 18mer:13mer template:primer (Chart 3). This monitored single nucleotide extension beyond the correctly inserted dC at the 3'-terminus of the primer. The polymerase was less efficient at extending nucleotides past the AFB<sub>1</sub>-β-FAPY adduct, as compared to the AFB<sub>1</sub>-N7-dG adduct. It did not efficiently insert any dNTP in the single-nucleotide extension reactions, although again in the dATP lanes, weak bands probably correspond to multiple insertions of dATP opposite the 5'-neighboring dT nucleotides in the template. When all four dNTPs were included, the primer was extended to the full-length 18-mer product.

These data recapitulated aspects of the site-specific mutagenesis for the AFB<sub>1</sub>-N7-dG and AFB<sub>1</sub>-FAPY adducts (37, 40). Predominantly error-free bypass was observed for the AFB<sub>1</sub>-N7-dG adduct (Figure 3), which correlated with the lower mutagenicity of this adduct (40). For the AFB<sub>1</sub>-N7-dG adduct the polymerase both inserted the correct dCTP opposite the damaged base and in the presence of all four dNTPs, extended the primer to a full-length product (Figure 3). With the AFB<sub>1</sub>-β-FAPY adduct, replication bypass was less efficient and error-prone, correlating with the greater mutagenicity of this adduct (Figure 4) (37). Also, the polymerase misincorporated dATP, albeit inefficiently, when challenged by the AFB<sub>1</sub>-β-FAPY adduct (Figure 4). This would be anticipated to lead to a G→T transversion, in agreement with site-specific mutagenesis studies (37).

### **Crystallography of AFB<sub>1</sub>-Adducted Template:Primers Complexed with the Dpo4 Polymerase**

Structures of the Dpo4 polymerase in complex with DNA and incoming dNTPs provide models for investigating the structural features that determine lesion bypass efficiency and fidelity with the corresponding human Y-family polymerases (58). The active sites of Y-family polymerases are solvent accessible and in some cases can accommodate two template bases (58-63). The nascent base pair is less constrained than for replicative polymerases. The spacious active site relaxes geometric selection for the incoming dNTP (60), compromising the efficiency and fidelity of replication. The bypass ability, accuracy, and efficiencies of these polymerases vary (57, 64-67) and depend on the types of DNA adduct (68-78).

The ternary complex of the AFB<sub>1</sub>-N7-dG adduct with the Sequence I 12-mer primer, showing correct insertion of dCTP opposite the adducted guanine (Figure 5) provided the first glimpse of the AFB<sub>1</sub>-N7-dG adduct during

replication bypass (56). The intercalation of the AFB<sub>1</sub> moiety above the 5'-face of the adducted guanine, with the methoxy group facing the minor groove of the template, and the two keto oxygens facing into the nascent duplex, was similar to that observed in DNA (55). The damaged nucleotide was accommodated within the active site of the polymerase without changes to the conformation of the AFB<sub>1</sub> adduct in DNA. The adducted guanine base and AFB<sub>1</sub> moiety were 16° out of plane. This was a consequence of maintaining the bond between N7-dG and the C8 carbon of the AFB<sub>1</sub> moiety in plane with the damaged guanine base and had been inferred from NMR data (44, 54). This allowed for stacking of the AFB<sub>1</sub> moiety above the 5'-face of the adducted guanine base, but created a wedge in the DNA. During bypass, this perhaps facilitates the insertion of the incoming dCTP between the AFB<sub>1</sub> moiety and the adducted guanine. The potential for Watson-Crick hydrogen bonding between the incoming dCTP and the guanine base remained intact (Figure 5). The distance between the 3'-OH group of the primer to the α-phosphate suggested an active complex. This may account for the ability of the polymerase to correctly insert dCTP opposite the AFB<sub>1</sub>-N7-dG lesion (Figure 3), consistent with the low mutagenicity of this lesion in *E. coli* (2, 40).

Figure 6 shows the polymerase active site, with the correct incoming dATP placed opposite to the template 5'-neighbor dT (56). The incoming dATP stacked above the AFB<sub>1</sub> moiety and was positioned to form Watson-Crick hydrogen bonds with the template dT (Figure 6). Watson-Crick base pairing was maintained between the guanine base of the AFB<sub>1</sub>-N7-dG adduct and the primer 3'-terminus dC. Both the guanine base and dC of the primer tilted out of plane toward the 3'-direction of the template. The AFB<sub>1</sub> moiety remained intercalated above the 5'-face of the modified guanine. The distance between the α-phosphate of the incoming dATP and the 3'-OH group of the primer was 6.7 Å.

Figure 7 shows the binary complex formed between the template containing the AFB<sub>1</sub>-FAPY adduct and Sequence II, the 13-mer primer (Chart 3) (56). The AFB<sub>1</sub> moiety intercalated above the 5'-face of the FAPY base. Similar to the AFB<sub>1</sub>-N7-dG lesion, this placed the methoxy group facing the minor groove of the template, with the two keto oxygens of AFB<sub>1</sub> facing the major groove of the template. The deoxyribose was in the β-anomeric configuration. The C5-N<sup>5</sup> bond of the pyrimidinyl moiety was in the R<sub>a</sub> configuration as observed for the AFB<sub>1</sub>-β-FAPY adduct in DNA (49, 53), and the nucleoside and the FAPY base (38). Rotation about this bond allowed the bond between the alkylated N<sup>5</sup> formamido nitrogen and the C8 of the AFB<sub>1</sub> moiety to orient out of plane with respect to the FAPY base and toward the 5'-direction, as had been inferred from NMR (49, 53, 55). This allowed the AFB<sub>1</sub> moiety to stack efficiently with the FAPY base. The 3'-primer terminus dC formed a Watson-Crick bonding interaction with the FAPY base. Unlike the binary complex involving native DNA (79) in which the primer terminus reached to the end of the active site,

here the site was occupied by the AFB<sub>1</sub>-β-FAPY adduct and the template 5'-neighbor dT (Figure 7). This was attributed to the intercalation of the AFB<sub>1</sub> moiety above the 5'-face of the FAPY base and the stacking of the AFB<sub>1</sub> moiety with the template 5'-neighbor dT. The distance between the primer terminus AFB<sub>1</sub>-FAPY:dC pair and AFB<sub>1</sub> was ~3.7 Å, similar to the helicoidal rise in B-DNA. The conformations of the protein side chains for Y10, Y48 and R51 were similar to those for the unmodified binary complex (79).

For the ternary complex showing correct insertion of dATP from the AFB<sub>1</sub>-β-FAPY:dC Sequence II primer (Chart 3) the AFB<sub>1</sub> moiety was parallel with the DNA base pairs and stacked between the FAPY base and 5'-neighbor dT (Figure 8) (56). The deoxyribose was in the β-anomeric configuration. The helicoidal rise between the AFB<sub>1</sub> moiety and the FAPY base was ~ 3.7 Å. The incoming dATP paired with the 5'-neighbor template base dT, with conservation of Watson-Crick hydrogen bonding (Figure 8). At the 3'-terminus of the primer, Watson-Crick hydrogen bonding was maintained between the FAPY base and the primer dC (Figure 8). This resulted in a gap of 6.9 Å between the 3'-hydroxyl of the primer dC and the α-phosphate of the dATP (Figure 8). The oxygen atom of the formamide group participated in a water-mediated hydrogen bond with Arg332 and made van der Waals contacts with Ile 295. Three bound Ca<sup>2+</sup> ions were identified (Figure 8). The first two were in the active site for catalysis and dNTP coordination. The third Ca<sup>2+</sup> ion was 3.0 Å from the side chain carbonyl oxygen of Ala181 in the thumb domain of the polymerase. One Ca<sup>2+</sup> ion at the active site was 3.5 Å distant from the primer 3'-terminus hydroxyl, suggesting that it was positioned to catalyze the reaction.

### Structure-Activity Relationships

The conformational differences of the AFB<sub>1</sub> moiety within the active site of the Dpo4 polymerase, which result from the differing orientations of the N7-C8 bond of the AFB<sub>1</sub>-N7-dG *vs.* the N<sup>5</sup>-C8 bond of the AFB<sub>1</sub>-β-FAPY adduct may, in part, modulate AFB<sub>1</sub> lesion bypass by this polymerase. For the AFB<sub>1</sub>-β-FAPY adduct, the parallel stacking of the AFB<sub>1</sub> moiety with the FAPY base may hinder access to the incoming dNTP (Figure 7). For the AFB<sub>1</sub>-N7-dG adduct, the adducted guanine base and AFB<sub>1</sub> moieties are 16° out of plane. The resulting wedge between the adducted guanine base and the AFB<sub>1</sub> moiety might facilitate access for the incoming dCTP (Figure 5), consistent with the error-free bypass of the AFB<sub>1</sub>-N7-dG adduct (Figure 3) (56).

The data suggest that following correct incorporation of dCTP opposite the AFB<sub>1</sub>-β-FAPY adduct, the polymerase can insert dATP opposite the template 5'-neighbor dT. In the ternary complex with the Sequence II 13-mer primer and incoming dATP the FAPY base conserves Watson-Crick hydrogen bonds with the 3'-primer terminus dC (Figure 8). The incoming dATP forms Watson-Crick hydrogen bonds with the template 5'-neighbor dT. The structure

seems unlikely to be catalytically competent since the distance between the 3'-OH of the primer and the  $\alpha$ -phosphate of the incoming dATP is more than 6.9 Å. It is unclear what rearrangements might facilitate phosphodiester bond formation although one could envision transient dynamics bringing these atoms sufficiently close to allow this. The incorporation of dATP opposite the template 5'-neighbor dT is reminiscent of the "Type II" structure observed for ternary complexes of the polymerase with undamaged DNA (58). The polymerase accommodates two template nucleotides, and it inserts the dATP opposite the template 5'-neighbor nucleotide, rather than the damaged nucleotide. Remarkably, the active site accommodates the FAPY base, the AFB<sub>1</sub> moiety, and the template 5'-neighbor dT. Thus, this could be considered to be a "pseudo" Type II structure (56).

## Summary

Progress has been made in understanding the DNA chemistry associated with human exposures to the mycotoxin AFB<sub>1</sub>. Both the initially formed AFB<sub>1</sub>-N7-dG adduct and its rearrangement product, the AFB<sub>1</sub>-FAPY adduct, exhibit intercalation of the AFB<sub>1</sub> moiety above the 5'-face of the damaged base. Site-specific mutagenesis conducted in *E. coli* shows that both the AFB<sub>1</sub>-N7-dG and the AFB<sub>1</sub>-FAPY adducts are mutagenic and induce G→T transversions. However, the AFB<sub>1</sub>-FAPY adduct is significantly more mutagenic. Crystallographic studies using site-specifically modified template:primers with the Y-family Dpo4 polymerase indicate that conformational differences of the AFB<sub>1</sub> moiety within the active site of the polymerase, which result from the differing orientations of the N7-C8 bond of the AFB<sub>1</sub>-N7-dG vs. the N<sup>5</sup>-C8 bond of the AFB<sub>1</sub>-β-FAPY adduct may, in part, modulate AFB<sub>1</sub> adduct bypass. Future studies will examine the site-specific mutagenesis of these adducts in mammalian cells and the replication bypass of these adducts by human Y-family polymerases.

## Laboratory Safety Statement

AFB<sub>1</sub> is a potent liver toxin and is genotoxic, and it should be presumed that AFB<sub>1</sub>-exo-8,9-epoxide is toxic and genotoxic. Crystalline aflatoxins are hazardous due to their electrostatic nature. AFB<sub>1</sub> can be destroyed by oxidation with NaOCl. Manipulations should be carried out in a well-ventilated hood with suitable containment procedures.

## Data Deposition

Complete structure factor and final coordinates were deposited in the Protein Data Bank ([www.rcsb.org](http://www.rcsb.org)): PDB ID codes for the ternary complexes of

the AFB<sub>1</sub>-N7-dG adduct with dCTP, 3PW7; with dATP, 3PW4; for the binary complex of the AFB<sub>1</sub>-β-FAPY, 3PVX; for the ternary complex of the AFB<sub>1</sub>-β-FAPY adduct with dATP, 3PW0.

## Acknowledgements

This work was presented, in part, at the 66<sup>th</sup> Southwestern Regional Meeting and 62<sup>nd</sup> Southeastern Regional Meeting of the American Chemical Society, New Orleans, Louisiana, December 2010. This work was funded by NIH grants R01 CA-55678 (M.P.S.), the Vanderbilt University Center in Molecular Toxicology, P30 ES-00267, and the Vanderbilt-Ingram Cancer Center, P30 CA-68485. Vanderbilt University and the Vanderbilt Center for Structural Biology assisted with the purchase of in-house crystallographic instrumentation. Crystallographic data were collected on the 21-ID-F beamline of the Life Sciences Collaborative Access Team (LS-CAT) at the Advanced Photon Source (Argonne National Laboratory, Argonne, IL). Supporting institutions may be found at <http://ls-cat.org/members.html>. Use of the Advanced Photon Source was supported by the U.S. Department of Energy, Basic Energy Sciences, Office of Science, under Contract W-31109-Eng-38.

## References

1. Busby Jr., W. F.; Wogan, G. N., Aflatoxins. In *Chemical Carcinogens*, 2<sup>nd</sup> Ed.; Searle, C. E., Ed. American Chemical Society: Washington, D.C., 1984; pp 945-1136.
2. Smela, M. E.; Currier, S. S.; Bailey, E. A.; Essigmann, J. M. *Carcinogenesis* **2001**, *22*, 535-545.
3. Bennett, J. W.; Klich, M. *Clin. Microbiol. Rev.* **2003**, *16*, 497-516.
4. Kensler, T. W.; Roebuck, B. D.; Wogan, G. N.; Groopman, J. D. *Toxicol. Sci.* **2011**, *120 Suppl 1*, S28-48.
5. McCann, J.; Spingarn, N. E.; Koburi, J.; Ames, B. N. *Proc. Natl. Acad. Sci. USA* **1975**, *72*, 979-983.
6. Foster, P. L.; Eisenstadt, E.; Miller, J. H. *Proc. Natl. Acad. Sci. USA* **1983**, *80*, 2695-2698.
7. Foster, P. L.; Groopman, J. D.; Eisenstadt, E. *J. Bacteriol.* **1988**, *170*, 3415-3420.
8. Bailey, G. S.; Williams, D. E.; Wilcox, J. S.; Loveland, P. M.; Coulombe, R. A.; Hendricks, J. D. *Carcinogenesis* **1988**, *9*, 1919-1926.
9. Bailey, G. S.; Loveland, P. M.; Pereira, C.; Pierce, D.; Hendricks, J. D.; Groopman, J. D. *Mutat. Res.* **1994**, *313*, 25-38.
10. McMahon, G.; Davis, E. F.; Huber, L. J.; Kim, Y.; Wogan, G. N. *Proc. Natl. Acad. Sci. USA* **1990**, *87*, 1104-1108.

11. Soman, N. R.; Wogan, G. N. *Proc. Natl. Acad. Sci. USA* **1993**, *90*, 2045-2049.
12. Yang, M.; Zhou, H.; Kong, R. Y.; Fong, W. F.; Ren, L. Q.; Liao, X. H.; Wang, Y.; Zhuang, W.; Yang, S. *Mutat. Res.* **1997**, *381*, 25-29.
13. Groopman, J. D.; Kensler, T. W. *Toxicol. Appl. Pharmacol.* **2005**, *206*, 131-137.
14. Kensler, T. W.; Roebuck, B. D.; Wogan, G. N.; Groopman, J. D. *Toxicol. Sci.* **2010**.
15. Bressac, B.; Kew, M.; Wands, J.; Ozturk, M. *Nature* **1991**, *350*, 429-431.
16. Hsu, I. C.; Metcalf, R. A.; Sun, T.; Welsh, J. A.; Wang, N. J.; Harris, C. C. *Nature* **1991**, *350*, 427-428.
17. Greenblatt, M. S.; Bennett, W. P.; Hollstein, M.; Harris, C. C. *Cancer Res.* **1994**, *54*, 4855-4878.
18. Shen, H. M.; Ong, C. N. *Mutat. Res.* **1996**, *366*, 23-44.
19. Soini, Y.; Chia, S. C.; Bennett, W. P.; Groopman, J. D.; Wang, J. S.; DeBenedetti, V. M.; Cawley, H.; Welsh, J. A.; Hansen, C.; Bergasa, N. V.; Jones, E. A.; DiBisceglie, A. M.; Trivers, G. E.; Sandoval, C. A.; Calderon, I. E.; Munoz Espinosa, L. E.; Harris, C. C. *Carcinogenesis* **1996**, *17*, 1007-1012.
20. Lunn, R. M.; Zhang, Y. J.; Wang, L. Y.; Chen, C. J.; Lee, P. H.; Lee, C. S.; Tsai, W. Y.; Santella, R. M. *Cancer Res.* **1997**, *57*, 3471-3477.
21. Mace, K.; Aguilar, F.; Wang, J. S.; Vautravers, P.; Gomez-Lechon, M.; Gonzalez, F. J.; Groopman, J.; Harris, C. C.; Pfeifer, A. M. *Carcinogenesis* **1997**, *18*, 1291-1297.
22. Shimada, T.; Guengerich, F. P. *Proc. Natl. Acad. Sci. USA* **1989**, *86*, 462-465.
23. Raney, K. D.; Shimada, T.; Kim, D. H.; Groopman, J. D.; Harris, T. M.; Guengerich, F. P. *Chem. Res. Toxicol.* **1992**, *5*, 202-210.
24. Ueng, Y. F.; Shimada, T.; Yamazaki, H.; Guengerich, F. P. *Chem. Res. Toxicol.* **1995**, *8*, 218-225.
25. Gallagher, E. P.; Kunze, K. L.; Stapleton, P. L.; Eaton, D. L. *Toxicol. Appl. Pharmacol.* **1996**, *141*, 595-606.
26. Johnson, W. W.; Harris, T. M.; Guengerich, F. P. *J. Am. Chem. Soc.* **1996**, *118*, 8213-8220.
27. Baertschi, S. W.; Raney, K. D.; Stone, M. P.; Harris, T. M. *J. Am. Chem. Soc.* **1988**, *110*, 7929-7931.
28. Murray, R. W.; Jeyaraman, R. *J. Org. Chem.* **1985**, *50*, 2847-2853.
29. Adam, W.; Bialas, J.; Hadjiarapoglou, L. *Chem. Ber.* **1991**, *124*, 2377-2377.
30. Essigmann, J. M.; Croy, R. G.; Nadzan, A. M.; Busby Jr., W. F.; Reinhold, V. N.; Buchi, G.; Wogan, G. N. *Proc. Natl. Acad. Sci. USA* **1977**, *74*, 1870-1874.
31. Gopalakrishnan, S.; Byrd, S.; Stone, M. P.; Harris, T. M. *Biochemistry* **1989**, *28*, 726-734.

32. Iyer, R. S.; Coles, B. F.; Raney, K. D.; Thier, R.; Guengerich, F. P.; Harris, T. M. *J. Am. Chem. Soc.* **1994**, *116*, 1603-1609.
33. Hertzog, P. J.; Smith, J. R. L.; Garner, R. C. *Carcinogenesis* **1982**, *3*, 723-725.
34. Hertzog, P. J.; Lindsay Smith, J. R.; Garner, R. C. *Carcinogenesis* **1980**, *1*, 787-793.
35. Croy, R. G.; Wogan, G. N. *Cancer Res.* **1981**, *41*, 197-203.
36. Groopman, J. D.; Croy, R. G.; Wogan, G. N. *Proc. Natl. Acad. Sci. USA* **1981**, *78*, 5445-5449.
37. Smela, M. E.; Hamm, M. L.; Henderson, P. T.; Harris, C. M.; Harris, T. M.; Essigmann, J. M. *Proc. Natl. Acad. Sci. USA* **2002**, *99*, 6655-6660.
38. Brown, K. L.; Deng, J. Z.; Iyer, R. S.; Iyer, L. G.; Voehler, M. W.; Stone, M. P.; Harris, C. M.; Harris, T. M. *J. Am. Chem. Soc.* **2006**, *128*, 15188-15199.
39. Essigmann, J. M.; Fowler, K. W.; Green, C. L.; Loechler, E. L. *Environ. Health Perspect.* **1985**, *62*, 171-6.
40. Bailey, E. A.; Iyer, R. S.; Stone, M. P.; Harris, T. M.; Essigmann, J. M. *Proc. Natl. Acad. Sci. USA* **1996**, *93*, 1535-1539.
41. Reid, B. R. *Q. Rev. Biophys.* **1987**, *20*, 2-28.
42. Patel, D. J.; Shapiro, L.; Hare, D. *Q. Rev. Biophys.* **1987**, *20*, 35-112.
43. Gopalakrishnan, S.; Harris, T. M.; Stone, M. P. *Biochemistry* **1990**, *29*, 10438-10448.
44. Jones, W. R.; Johnston, D. S.; Stone, M. P. *Chem. Res. Toxicol.* **1998**, *11*, 873-881.
45. Giri, I.; Jenkins, M. D.; Schnetz-Boutaud, N. C.; Stone, M. P. *Chem. Res. Toxicol.* **2002**, *15*, 638-647.
46. Johnston, D. S.; Stone, M. P. *Biochemistry* **1995**, *34*, 14037-14050.
47. Gopalakrishnan, S.; Liu, X.; Patel, D. J. *Biochemistry* **1992**, *31*, 10790-10801.
48. Gopalakrishnan, S.; Stone, M. P.; Harris, T. M. *J. Am. Chem. Soc.* **1989**, *111*, 7232-7239.
49. Giri, I.; Stone, M. P. *Biopolymers* **2002**, *65*, 190-201.
50. Alekseyev, Y. O.; Hamm, M. L.; Essigmann, J. M. *Carcinogenesis* **2004**, *25*, 1045-1051.
51. Tainer, J. A. *Prog. Nucleic Acid Res. Mol. Biol.* **2001**, *68*, 299-304.
52. Min, J. H.; Pavletich, N. P. *Nature* **2007**, *449*, 570-575.
53. Mao, H.; Deng, Z.; Wang, F.; Harris, T. M.; Stone, M. P. *Biochemistry* **1998**, *37*, 4374-4387.
54. Giri, I.; Jenkins, M. D.; Schnetz-Boutaud, N. C.; Stone, M. P. *Chem. Res. Toxicol.* **2002**, *15*, 638-647.
55. Brown, K. L.; Voehler, M. W.; Magee, S. M.; Harris, C. M.; Harris, T. M.; Stone, M. P. *J. Am. Chem. Soc.* **2009**, *131*, 16096-16107.

56. Banerjee, S.; Brown, K. L.; Egli, M.; Stone, M. P. *manuscript in preparation*.
57. Boudsocq, F.; Iwai, S.; Hanaoka, F.; Woodgate, R. *Nucleic Acids Res.* **2001**, *29*, 4607-4616.
58. Ling, H.; Boudsocq, F.; Woodgate, R.; Yang, W. *Cell* **2001**, *107*, 91-102.
59. Silvan, L. F.; Toth, E. A.; Pham, P.; Goodman, M. F.; Ellenberger, T. *Nat. Struct. Biol.* **2001**, *8*, 984-989.
60. Goodman, M. F. *Annu. Rev. Biochem.* **2002**, *71*, 17-50.
61. Alt, A.; Lammens, K.; Chiocchini, C.; Lammens, A.; Pieck, J. C.; Kuch, D.; Hopfner, K. P.; Carell, T. *Science* **2007**, *318*, 967-70.
62. Reissner, T.; Schneider, S.; Schorr, S.; Carell, T. *Angewandte Chemie (International Ed)* **2010**, *49*, 3077-3080.
63. Silverstein, T. D.; Johnson, R. E.; Jain, R.; Prakash, L.; Prakash, S.; Aggarwal, A. K. *Nature* **2010**, *465*, 1039-1043.
64. Johnson, R. E.; Prakash, S.; Prakash, L. *Proc. Natl. Acad. Sci. USA* **2000**, *97*, 3838-3843.
65. Zhang, Y.; Yuan, F.; Wu, X.; Rechkoblit, O.; Taylor, J. S.; Geacintov, N. E.; Wang, Z. *Nucleic Acids Res.* **2000**, *28*, 4717-4724.
66. Ohashi, E.; Bebenek, K.; Matsuda, T.; Feaver, W. J.; Gerlach, V. L.; Friedberg, E. C.; Ohmori, H.; Kunkel, T. A. *J. Biol. Chem.* **2000**, *275*, 39678-39684.
67. Gerlach, V. L.; Feaver, W. J.; Fischhaber, P. L.; Friedberg, E. C. *J. Biol. Chem.* **2001**, *276*, 92-98.
68. Johnson, R. E.; Prakash, S.; Prakash, L. *Science* **1999**, *283*, 1001-1004.
69. Ohashi, E.; Ogi, T.; Kusumoto, R.; Iwai, S.; Masutani, C.; Hanaoka, F.; Ohmori, H. *Genes Dev.* **2000**, *14*, 1589-1594.
70. Haracska, L.; Yu, S. L.; Johnson, R. E.; Prakash, L.; Prakash, S. *Nat. Genet.* **2000**, *25*, 458-461.
71. Johnson, R. E.; Washington, M. T.; Haracska, L.; Prakash, S.; Prakash, L. *Nature* **2000**, *406*, 1015-1019.
72. Frank, E. G.; Sayer, J. M.; Kroth, H.; Ohashi, E.; Ohmori, H.; Jerina, D. M.; Woodgate, R. *Nucleic Acids Res.* **2002**, *30*, 5284-5292.
73. Rechkoblit, O.; Zhang, Y.; Guo, D.; Wang, Z.; Amin, S.; Krzeminsky, J.; Louneva, N.; Geacintov, N. E. *J. Biol. Chem.* **2002**, *277*, 30488-30494.
74. Huang, X.; Kolbanovskiy, A.; Wu, X.; Zhang, Y.; Wang, Z.; Zhuang, P.; Amin, S.; Geacintov, N. E. *Biochemistry* **2003**, *42*, 2456-266.
75. Washington, M. T.; Minko, I. G.; Johnson, R. E.; Haracska, L.; Harris, T. M.; Lloyd, R. S.; Prakash, S.; Prakash, L. *Mol. Cell Biol.* **2004**, *24*, 6900-6906.
76. Washington, M. T.; Minko, I. G.; Johnson, R. E.; Wolfle, W. T.; Harris, T. M.; Lloyd, R. S.; Prakash, S.; Prakash, L. *Mol. Cell Biol.* **2004**, *24*, 5687-5693.

77. Rechkoblit, O.; Kolbanovskiy, A.; Malinina, L.; Geacintov, N. E.; Broyde, S.; Patel, D. J. *Nat. Struct. Mol. Biol.* **2010**, *17*, 379-388.
78. Wong, J. H.; Brown, J. A.; Suo, Z.; Blum, P.; Nohmi, T.; Ling, H. *EMBO J.* **2010**, *29*, 2059-2069.
79. Wong, J. H.; Fiala, K. A.; Suo, Z.; Ling, H. *J. Mol. Biol.* **2008**, *379*, 317-330.

## Figure Captions

**Chart 1.** Chemistry of AFB<sub>1</sub>-induced DNA alkylation. Cytochrome P450-mediated oxidation of AFB<sub>1</sub> forms aflatoxin B<sub>1</sub>-exo-8,9-epoxide, a reactive electrophile. This alkylates DNA regioselectively at the N7 position of guanine, forming the AFB<sub>1</sub>-N7-dG adduct. At neutral and acidic pH, this adduct is prone to depurination, but at basic pH, it converts to the AFB<sub>1</sub>-FAPY adduct.

**Chart 2.** Chemistry of the AFB<sub>1</sub>-FAPY adduct. **A.** Formation of the AFB<sub>1</sub>-FAPY adduct via base-catalyzed ring opening of the AFB<sub>1</sub>-N7-dG adduct. **B.** The AFB<sub>1</sub>-FAPY adduct interconverts between  $\alpha$  and  $\beta$  anomers; the equilibrium is dependent on single strand vs. duplex DNA environments. Note the change in atomic numbering of the AFB<sub>1</sub>-FAPY adducts, where the N7 nitrogen of guanine becomes the N<sup>5</sup> nitrogen of the AFB<sub>1</sub>-FAPY adducts. In nucleosides and nucleotides, two atropomers, R<sub>a</sub> and S<sub>a</sub>, are possible about the AFB<sub>1</sub>-FAPY C5-N<sup>5</sup> bond. Furthermore, Z and E geometrical isomers are possible about the formamide bond. In duplex DNA, rotation about the C5-N<sup>5</sup> bond is restricted because of the intercalated AFB<sub>1</sub> moiety, and the R<sub>a</sub> atropisomer predominates.

**Chart 3.** Sequences used for gel extension assays and crystallography. **Top:** The 12-mer Sequence I primer used for examining insertion of dNTPs opposite the AFB<sub>1</sub> adducts. **Bottom:** The 13-mer Sequence II primer used for examining extension of dNTPs opposite either the AFB<sub>1</sub>-N7-dG:dC or AFB<sub>1</sub>-FAPY:dC base pairs. X denotes either the AFB<sub>1</sub>-N7-dG or AFB<sub>1</sub>- $\beta$ -FAPY adducts.

**Figure 1.** Structure of the AFB<sub>1</sub>-N7-dG adduct in the 5'-d(CXA)-3':5'-d(TCG)-3' sequence as determined by NMR; X = AFB<sub>1</sub>-N7-dG adduct. The adduct intercalates above the 5'-face of the modified guanine base and increases the thermal melting temperature (T<sub>m</sub>) of the duplex.

**Figure 2.** Structure of the AFB<sub>1</sub>- $\beta$ -FAPY adduct in the modified 5'-d(TXA)-3':5'-d(TCA)-3' sequence as determined by NMR; X = AFB<sub>1</sub>- $\beta$ -FAPY adduct. The adduct intercalates

above the 5'-face of the modified guanine and increases the thermal melting temperature ( $T_m$ ) of the duplex. The arrow indicates the positioning of the formamide moiety in the major groove.

**Figure 3.** Replication bypass of the AFB<sub>1</sub>-N7-dG modified Sequence I and Sequence II template:primers with *S. solfataricus* P2 DNA polymerase Dpo4. The sequences I and II are displayed with the gels. The concentrations of the dNTPs are provided below the gels. The designations A, T, C, G represent single nucleotide incorporation experiments; the designation ALL represents the full-length extension assay incorporating all four dNTPs. Each assay was incubated for 1 hr at 37 °C.

**Figure 4.** Replication bypass of the AFB<sub>1</sub>-β-FAPY modified Sequence I and Sequence II template:primers with *S. solfataricus* P2 DNA polymerase Dpo4. The sequences I and II are displayed with the gels. The concentrations of the dNTPs are provided below the gels. The designations A, T, C, G represent single nucleotide incorporation experiments; the designation ALL represents the full-length extension assay incorporating all four dNTPs. Each assay was incubated for 1 hr at 37 °C.

**Figure 5.** Structure of the ternary AFB<sub>1</sub>-N7-dG modified Sequence I template:primer complex with the *S. solfataricus* P2 DNA polymerase Dpo4 and incoming dCTP. **A.** Electron density at the active site. **B.** Watson-Crick base pair between AFB<sub>1</sub>-N7-dG and 3'-primer terminus dC. **C.** Watson-Crick dA:dT base pair involving the template 3'-neighbor dA. **D.** Active site with the modified template:primer and the dCTP along with the polymerase. The Dpo4 is colored green and the AFB<sub>1</sub>-N7-dG adduct is colored cyan.

**Figure 6.** Structure of the ternary AFB<sub>1</sub>-N7-dG modified Sequence II template:primer complex with the *S. solfataricus* P2 DNA polymerase Dpo4 and incoming dATP. **A.** Electron density at the active site. **B.** Watson-Crick base pair between the 5'-template neighbor T and incoming dATP. **C.** Watson-Crick base pair between AFB<sub>1</sub>-N7-dG and 3'-primer terminus dC. **D.** Active site with the modified template:primer and the dATP along with the polymerase. The Dpo4 is colored green

and the AFB<sub>1</sub>-N7-dG is colored cyan. The Ca<sup>2+</sup> ions are shown as blue spheres.

**Figure 7.** Structure of the binary AFB<sub>1</sub>-β-FAPY modified Sequence II template:primer complex with the *S. solfataricus* P2 DNA polymerase Dpo4. **A.** Electron density at the active site. **B.** Watson-Crick base pair between the FAPY base of the AFB<sub>1</sub>-β-FAPY adduct and 3'-primer terminus dC. **C.** The electron density of the AFB<sub>1</sub>-β-FAPY nucleoside. **D.** Active site with the modified template:primer along with the polymerase. The Dpo4 is colored green and the AFB<sub>1</sub>-N7-dG is colored cyan. The Ca<sup>2+</sup> ions are shown as blue spheres.

**Figure 8.** Structure of the ternary AFB<sub>1</sub>-β-FAPY modified Sequence II template:primer complex with the *S. solfataricus* P2 DNA polymerase Dpo4 and incoming dATP. **A.** Electron density at the active site. **B.** Watson-Crick base pair between the 5'-template T and the incoming dATP. **C.** Watson-Crick base pair between the FAPY base of the AFB<sub>1</sub>-β-FAPY adduct and 3'-primer terminus dC. **D.** Active site with the modified template:primer along with the polymerase and the dATP. The Dpo4 is colored green and the AFB<sub>1</sub>-β-FAPY is colored cyan. The Ca<sup>2+</sup> ions are shown as blue spheres.

Chart 1.

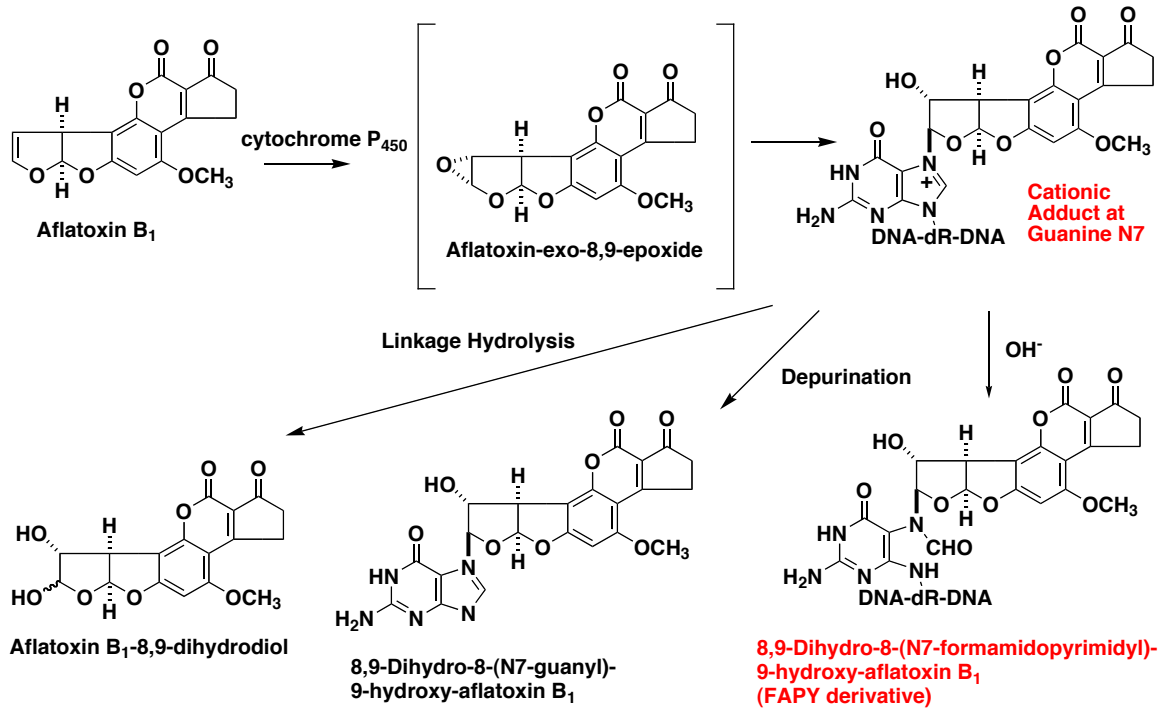


Chart 2.

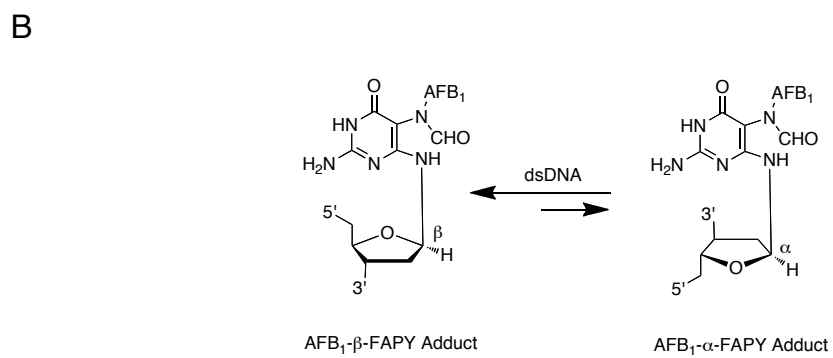
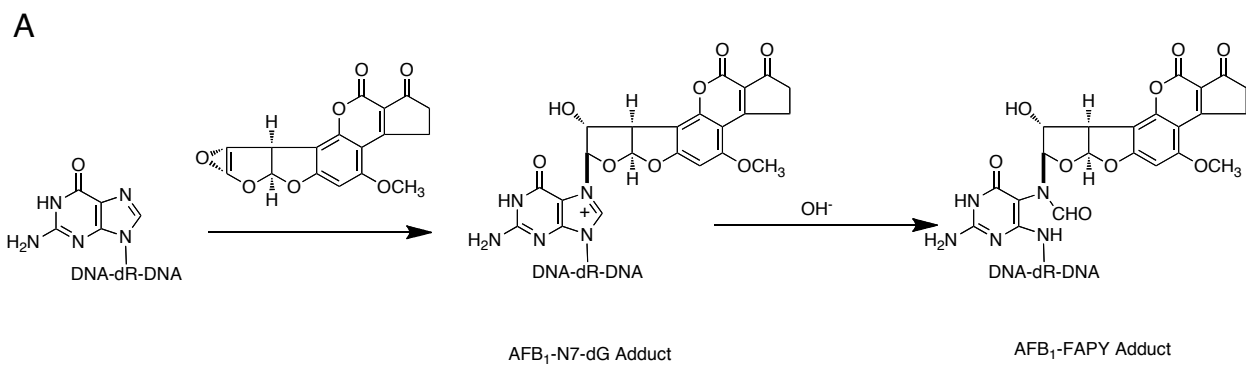


Chart 3

5' -GGGGGAAGGATT-3'  
3' -CCCCCTTCCTAAXTTACT-5'

5' -GGGGGAAGGATTC-3'  
3' -CCCCCTTCCTAAXTTACT-5'

Figure 1.

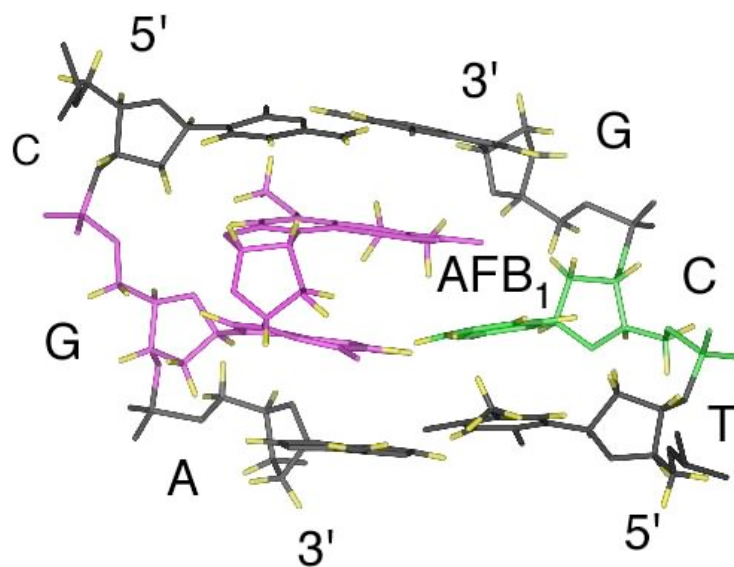


Figure 2.

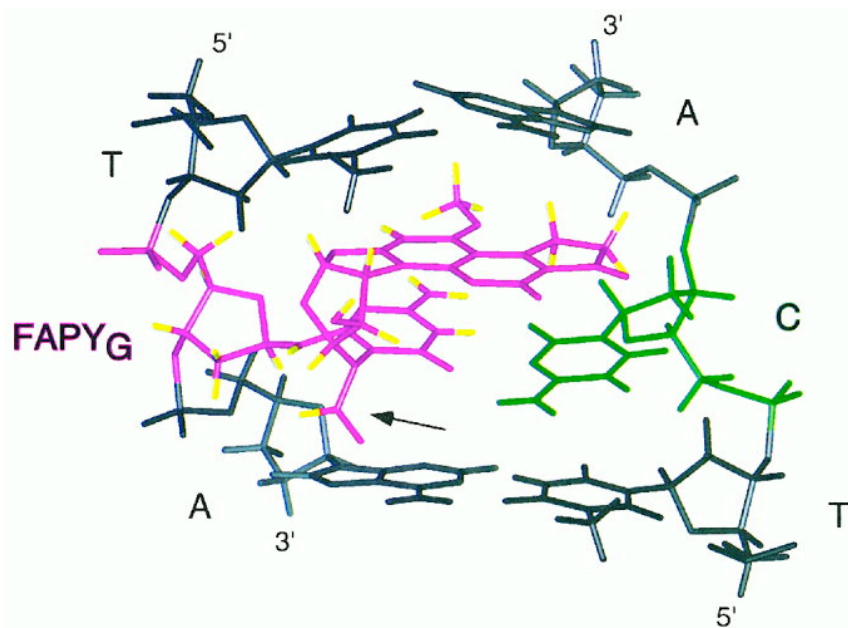


Figure 3

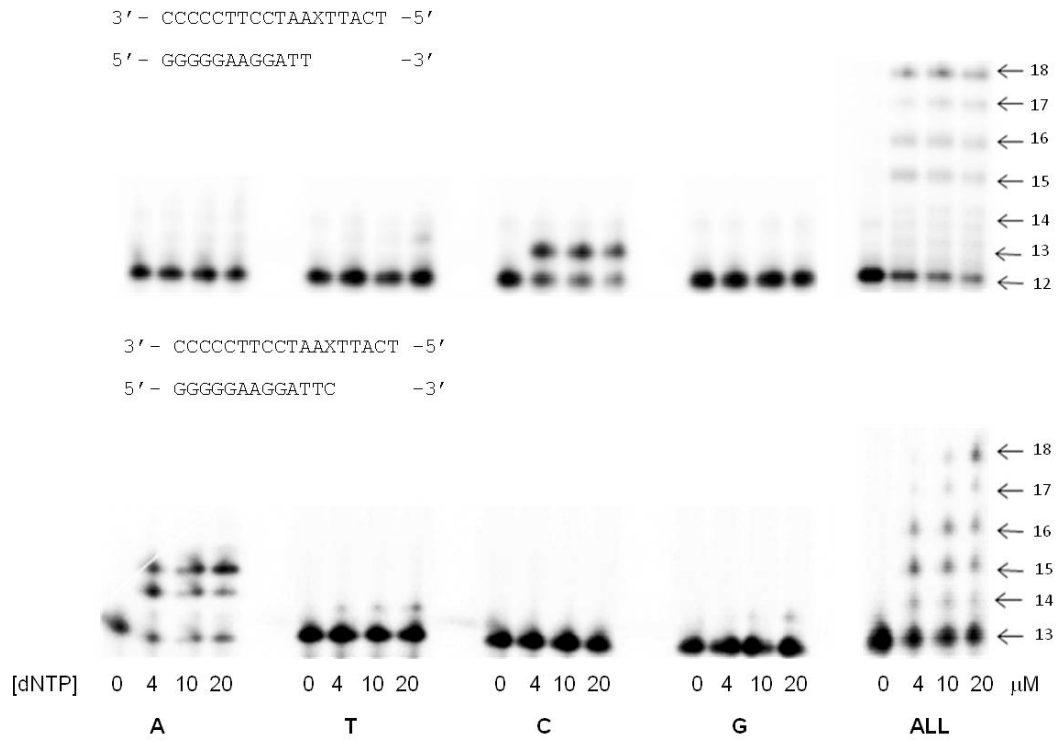


Figure 4

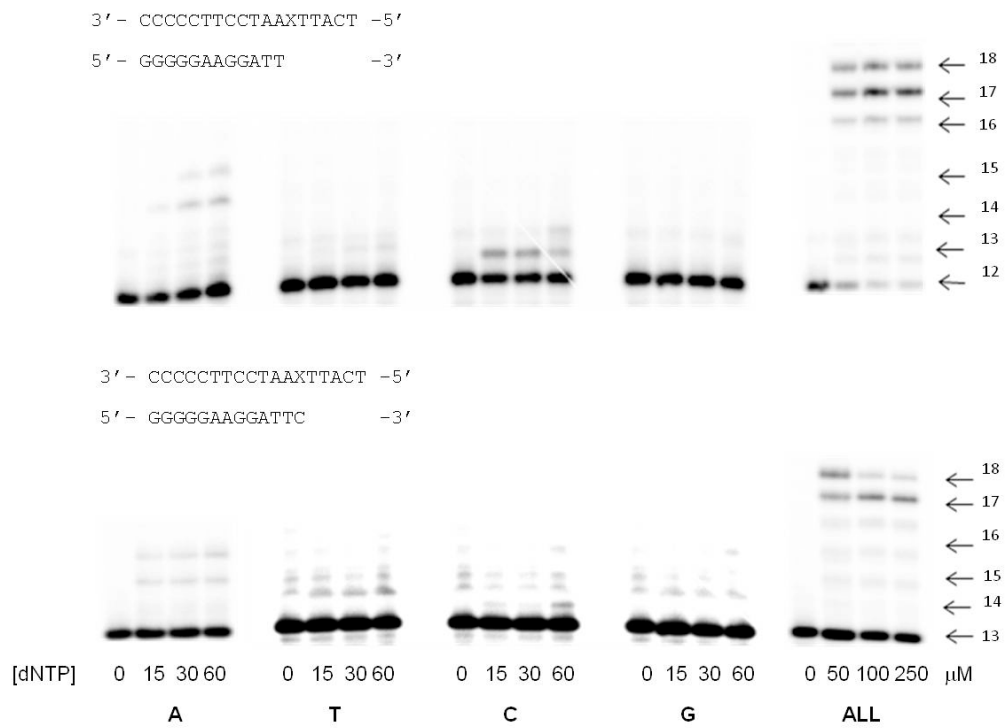


Figure 5

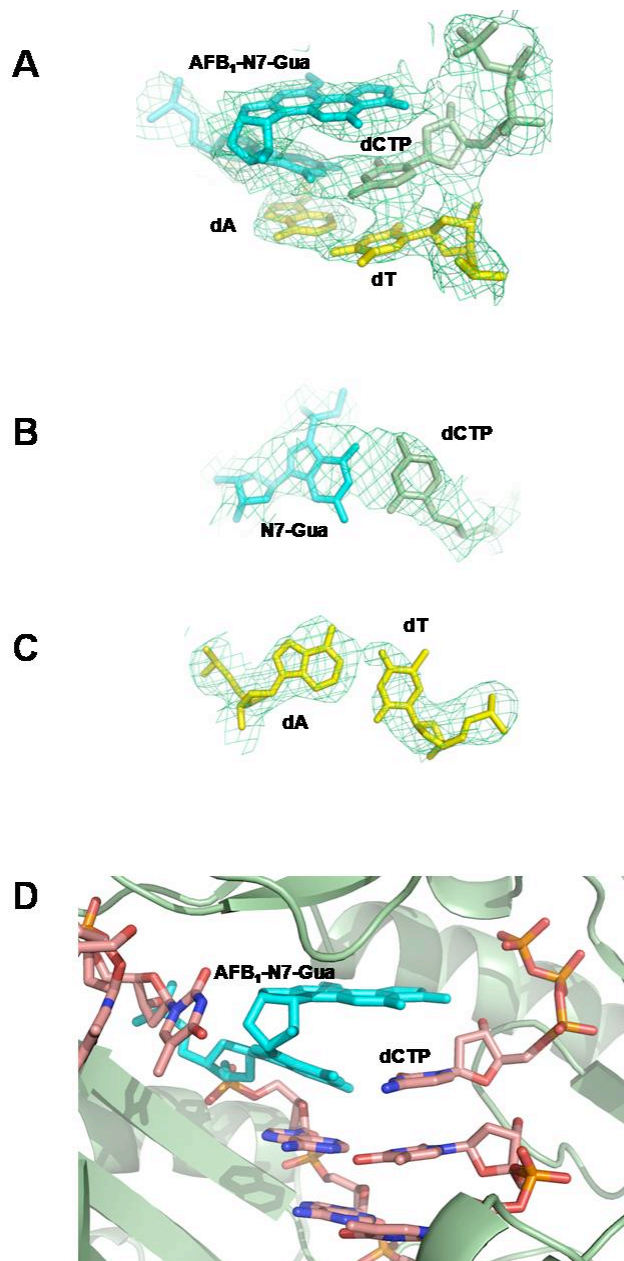


Figure 6

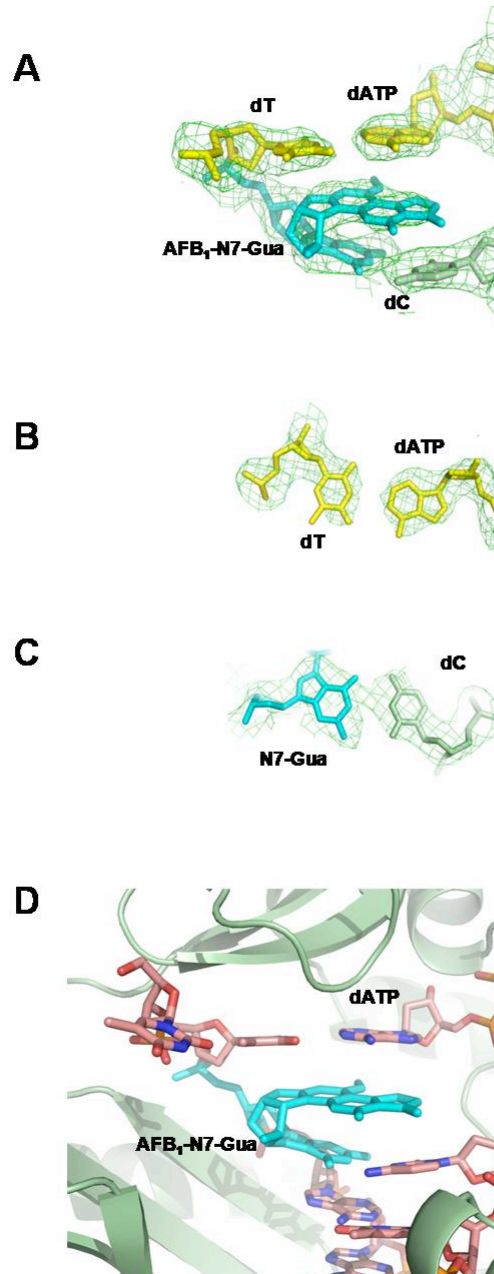


Figure 7

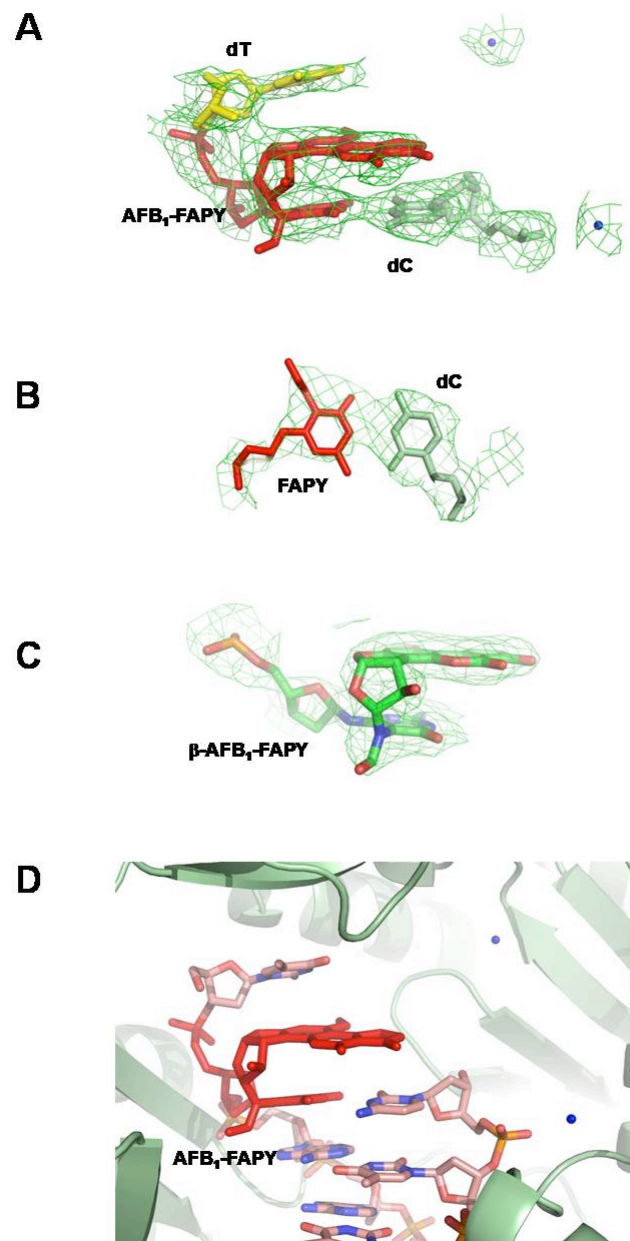


Figure 8

